Nanoscale

PAPER

View Article Online
View Journal | View Issue

Cite this: *Nanoscale*, 2020, **12**, 23234

A glycoconjugate-based gold nanoparticle approach for the targeted treatment of *Pseudomonas aeruginosa* biofilms†

Chao Zhang,‡[a] De-Tai Shi,‡[b,c] Kai-Cheng Yan, ‡[b,d] Adam C. Sedgwick, [e] Guo-Rong Chen,[b] Xiao-Peng He, [b] Tony D. James, [d] Bing Ye,*[a] Xi-Le Hu*[b] and Daijie Chen*[f]

In this study, "core–shell" gold nanoparticles (AuNPs) have been functionalised using a simple one-pot approach to form fucose-based glycoconjugate AuNPs (**Fuc-AuNPs**) and galactose-based glycoconjugate AuNPs (**Gal-AuNPs**), respectively. Owing to the selective carbohydrate-based recognition of the key virulence factors of *P. aeruginosa*, LecB (fucose-specific lectin)/LecA (galactose-specific lectin), **Fuc-AuNPs** and **Gal-AuNPs**-based imaging and therapeutic strategies were evaluated towards *P. aeruginosa*. Both **Fuc-AuNPs** and **Gal-AuNPs** were non-covalently loaded with the fluorophore dicyanomethylene 4*H*-pyran (DCM) to afford two highly selective fluorescence imaging agents for the visualisation of *P. aeruginosa*. The loading of **Fuc-AuNPs** and **Gal-AuNPs** with the known antibiotic Ceftazidime (CAZ) exhibited an enhanced therapeutic effect, illustrating the significance of this targeted drug delivery strategy. Exploiting the phototherapeutic properties of AuNPs, photoirradiation (600 nm) of **Fuc-AuNP@CAZ/Gal-AuNP@CAZ** provided both photothermal and photodynamic therapeutic (PTT/PDT) effects, which facilitated the release of CAZ. **Fuc-AuNP@CAZ** and **Gal-AuNP@CAZ** were shown to be effective photo/chemotherapeutics resulting in almost complete eradication of *P. aeruginosa* biofilms formed on clinically relevant surfaces (glass slides and steel surface).

Received 18th July 2020,
Accepted 7th November 2020

DOI: 10.1039/d0nr05365a

rsc.li/nanoscale

Introduction

Pseudomonas aeruginosa (*P. aeruginosa*) is a ubiquitous Gram negative bacterium that has become a real concern for hospital acquired infections.[1,2] It is recognised as the main cause of morbidity and mortality in critically ill, immunocompromised and cystic fibrosis (CF) patients.[3,4] Moreover, *P. aeruginosa* has the ability to form biofilms on mucosal surfaces and medical implant devices,[1] which provide favourable and protective conditions for bacterial survival against host defence mechanisms and aggressive antibiotic treatment.[1,5,6] As a direct result, this has led to a continued increase in resistant and multidrug-resistant (MDR) *P. aeruginosa* and a restriction in treatment options.[7] Therefore, *P. aeruginosa* is now considered as a major public health threat.[8–10]

Rapid advancements in material-based sciences has led to the identification of a range of drug delivery platforms with inherent diagnostic/therapeutic properties (*i.e.* photodynamic therapy/photothermal therapy (PDT/PTT)).[11–15] These systems have been demonstrated as effective anticancer and antimicrobial agents that can be activated by single or dual excitation wavelengths (*e.g.* 660 nm and 808 nm).[12,14,16–22] Researchers have continued to explore these platforms by incorporating additional antimicrobial metals such as copper (Cu) and silver (Ag).[23–27] Within the field of material sciences, gold nanoparticles (AuNPs) are of particular interest owing to their unique multifunctional and biocompatible properties.[11,28] The high surface area-to-volume ratio and ease of functionalisation of AuNPs has provided the capability to incorporate

[a]*Emergency Department, Jinan Children's Hospital, No. 23976 Jingshi Road, Jinan City, Shandong Province, Jinan, China. E-mail: 13583184890@163.com*
[b]*Key Laboratory for Advanced Materials and Joint International Research Laboratory of Precision Chemistry and Molecular Engineering, Feringa Nobel Prize Scientist Joint Research Center, School of Chemistry and Molecular Engineering, East China University of Science and Technology, 130 Meilong Rd., Shanghai 200237, China. E-mail: xlhu@ecust.edu.cn*
[c]*School of Materials Science and Engineering, Jingdezhen Ceramic Institute, Jingdezhen, 333403, China*
[d]*Department of Chemistry, University of Bath, Bath, BA2 7AY, U.K*
[e]*Department of Chemistry, The University of Texas at Austin, 105 E 24th street A5300, Austin, TX 78712-1224, USA*
[f]*School of Pharmacy, Shanghai Jiao Tong University, 800 Dongchuan Rd., Shanghai 200240, Minhang District, China. E-mail: cdj@sjtu.edu.cn*

†Electronic supplementary information (ESI) available: Synthetic procedures, ^{1}H, ^{13}C NMR, and mass spectra, UV-Vis and fluorescence spectroscopic analyses, and other materials. See DOI: 10.1039/d0nr05365a

‡These authors contributed equally to this work.

therapeutics or targeting ligand units (*i.e.* peptides, carbohydrates and genetic material) onto the surface of AuNPs through covalent/non-covalent interactions.[28–31] As a result, AuNPs provide an attractive platform for the effective delivery of functional molecules through active and passive targeting.[32] In conjunction, with their ability to selectively deliver therapeutic agents,[30,33,34] AuNPs have been shown as effective phototherapeutics with the production of cytotoxic ROS (PDT) and/or heat (PTT).[35–38] Despite these promising attributes, the application of AuNPs have been mostly directed towards the development of anticancer agents with minimal attention on their use as antimicrobials.[14,39] Therefore, we envisioned tailoring the design of AuNPs to target specific bacteria would allow the controlled and selective delivery of antibiotics. Moreover, in combination with PTT/PDT, we believed this would afford an effective antimicrobial platform with minimal off-target toxicities[30] and could reduce the potential to develop MDR bacteria.

A key step in the pathogenesis of *P. aeruginosa* is the adhesion of bacterial cells to human tissue,[40] which is believed to occur through the targeted recognition of mammalian glycoproteins by virulence factors such as lectins (LecA and LecB).[41] Exploiting the selective carbohydrate-based recognition of LecA (galactose specific) and LecB (fucose specific), we have developed two glycoconjugate-based AuNPs which were coated with the monosaccharides fucose (**Fuc-AuNPs**) and galactose (**Gal-AuNPs**), respectively (Scheme 1). NIR fluorophore, dicyanomethylene-4*H*-pyran (DCM)[42] loaded AuNPs (**Fuc-AuNP@DCM** and **Gal-AuNP@DCM**) afforded two highly selective imaging agents for the visualisation of *P. aeruginosa*. In addition, this result suggests binding with *P. aeruginosa* facilitates the release of the molecular cargo from the AuNPs. As a result, both **Fuc-AuNPs** and **Gal-AuNPs** were subsequently loaded with the antibiotic Ceftazidime (CAZ),[43] to afford the dual photo/chemotherapeutics, **Fuc-AuNP@CAZ** and **Gal-AuNP@CAZ**. This targeted lectin approach improved the therapeutic efficacy of CAZ and in combination with photoirradiation (600 nm), **Fuc-AuNP@CAZ** and **Gal-AuNP@CAZ** exhibited the effective destruction of the established *P. aeruginosa* biofilms on clinically relevant surfaces – glass slides and steel surfaces (Scheme 1).

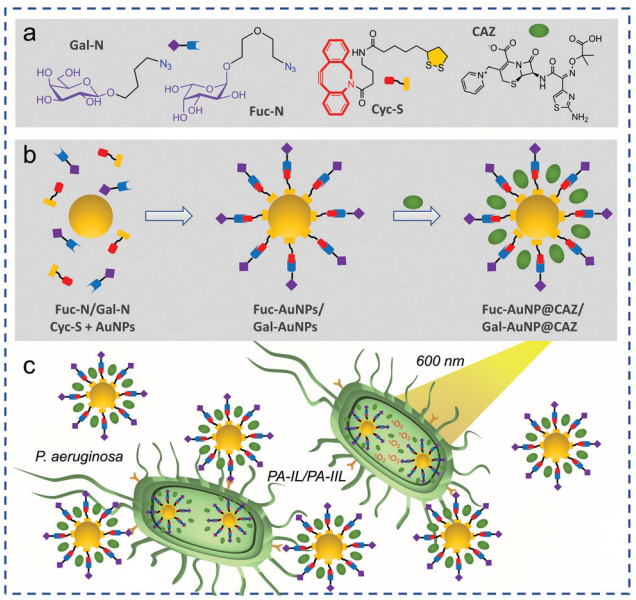

Scheme 1 (a) Key building blocks for the construction of **Fuc-AuNPs** and **Gal-AuNPs**: carbohydrate functionalised azide (Fuc-N and Gal-N) and cyclooctyne tailed disulfide ring (Cyc-S). Antibiotic as co-loaded molecular cargo: Ceftazidime (CAZ). (b) Schematic illustration of the one-pot self-assembly procedure and co-loading of CAZ to form **Fuc-AuNP@CAZ/Gal-AuNP@CAZ**. (c) Schematic illustration of the targeted lectin (LecB/LecA, also called PA-IIL/PA-IL) approach of **Fuc-AuNP@CAZ/Gal-AuNP@CAZ** to selectively enter *P. aeruginosa* to simultaneously release CAZ and generate ROS/heat upon photoirradiation (600 nm).

Copper-catalysed alkyne–azide cycloaddition (CuAAC) chemistry is routinely used for the synthesis of glycoconjugates.[44] Unfortunately, the use of Cu(I) ions for CuAAC chemistry can prove problematic for certain reaction substrates.[45] To overcome this limitation, strain-promoted "click" chemistry has been developed. In brief, a strained cyclooctyne unit covalently linked to a disulfide ring (Cyc-S) was used to form a self-assembled monolayer (SAM) on the surface of AuNPs.[46] Subsequent "click" chemistry between AuNP-Cyc-S (on the gold surface) and azide Fuc-N (fucosyl) or Gal-N (galactosyl) afforded the desired **Fuc-AuNPs** and **Gal-AuNPs** (see ESI† for the one-pot procedure). This was confirmed by a clear signal enhancement in the Raman spectrum (see ESI – Fig. S1†).[47,48] Moreover, zeta potential measurements demonstrated good aqueous stability for **Fuc-AuNPs** and **Gal-AuNPs** (see ESI – Fig. S1†).

With both **Fuc-AuNPs** and **Gal-AuNPs** in hand, the lectin binding properties of each AuNP was then evaluated. The addition of UEA-1 (Ulex European Agglutinin 1, fucose-specific lectin) to an aqueous solution of **Fuc-AuNPs** (0.2 nM) led to the broadening as well as a bathochromic shift of the UV-Vis absorption at 600 nm (Fig. 1a). This was attributed to aggregation of the AuNPs.[49,50] Minimal changes to the UV-vis absorption of **Fuc-AuNPs** were seen with the addition of other lectins/proteins (Fig. 1b), which was indicative of fucose selective binding. Similarly, the addition of PNA (Peanut Agglutinin, galactose-specific lectin) to a solution of **Gal-AuNPs** (0.2 nM) led to a gradual broadening as well as bathochromic shift of the UV-vis absorption at 600 nm (Fig. 1c and d). Again, minimal changes were observed when in the presence of other lectins/proteins. In addition, both **Fuc-AuNPs** and **Gal-AuNPs** demonstrated a high sensitivity for each corresponding lectin with low limit of detection (LoD) **Fuc-AuNPs** – UEA-1 = 13.8 nM/**Gal-AuNPs** – PNA = 4.9 nM (see ESI – Fig. S2†).

HR-TEM (High-Resolution Transmission Electron Microscope) images and Dynamic Light Scattering (DLS) analysis revealed no obvious differences between unmodified AuNPs and **Fuc-AuNPs**/**Gal-AuNPs** (Fig. 2 and Fig. S3†). However, in the presence of their corresponding lectins, both **Fuc-AuNPs** and **Gal-AuNPs** were shown to form large clusters, which was indicative of lectin binding and lectin-mediated

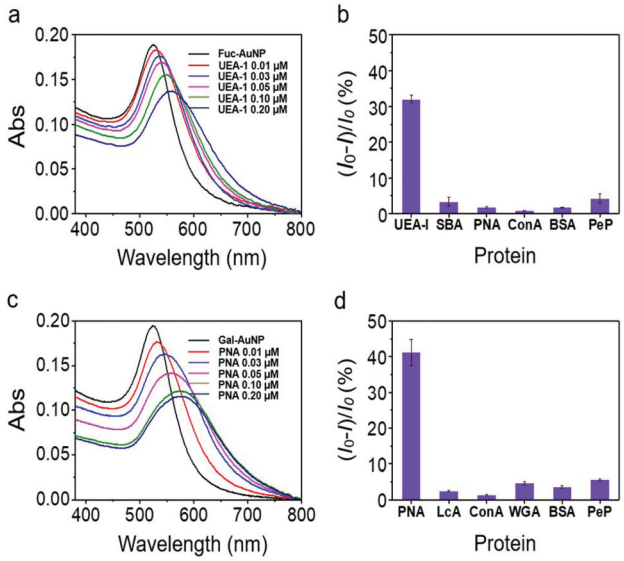

Fig. 1 (a) UV-vis spectra of **Fuc-AuNPs** (0.2 nM) with increasing concentrations of Ulex European Agglutinin 1 (UEA-1: 0.01–0.2 μM) in Tris-HCl buffer. (b) Change in UV-vis absorption at 525 nm of **Fuc-AuNPs** (0.2 nM) in the presence of UEA-1, SBA (Soybean Agglutinin), PNA, Con A (Conconvalin A), BSA (Bovine Serum Albumin), PeP (Pepsin) (protein concentrations: 0.05 μM). (c) UV-Vis spectra of **Gal-AuNPs** (0.2 nM) with increasing concentrations of Peanut Agglutinin (PNA: 0.01–0.2 μM) in Tris-HCl buffer. (d) Change in UV-Vis absorption at 525 nm of **Gal-AuNPs** (0.2 nM) in the presence of PNA, LcA (*Lens culinaris* Lectin), Con A (Conconvalin A), WGA (Wheat Germ Agglutinin), BSA (Bovine Serum Albumin), PeP (Pepsin) (Protein concentrations: 0.05 μM).

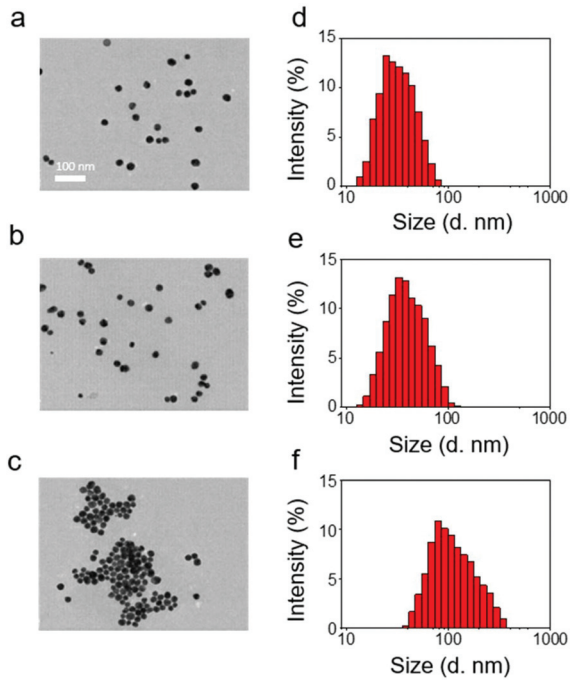

Fig. 2 High-Resolution Transmission Electron Microscope (HR-TEM) images: (a) AuNPs (0.02 nM) (b) **Fuc-AuNPs** (0.02 nM) (c) **Fuc-AuNPs** (0.02 nM) + UEA-1 (0.02 μM). Dynamic Light Scattering (DLS): (d) AuNPs (0.2 nM) (e) **Fuc-AuNPs** (0.2 nM) (f) **Fuc-AuNPs** (0.2 nM) + UEA-1 (0.05 μM).

agglutination (Fig. 2 and see ESI – Fig. S3 and S4†).[51] In addition, this further supported the lectin-mediated changes observed in the UV-Vis absorption of **Fuc-AuNPs** and **Gal-AuNPs** shown in Fig. 1a and c.

Upon identifying the lectin-binding properties of **Fuc-AuNPs** and **Gal-AuNPs**, the drug loading and phototherapeutic properties were then evaluated. **Fuc-AuNPs** or **Gal-AuNPs** (0.8 nM) were mixed in an aqueous solution containing CAZ for 4 h. Subsequent centrifugation (10 000 rpm) and washing (Tris-HCl buffer) afforded both **Fuc-AuNP@CAZ** and **Gal-AuNP@CAZ**. Both the loading of CAZ and corresponding **AuNP@CAZ** nanoparticle stability was confirmed by Raman spectroscopy and zeta potential measurements, respectively (see ESI – Fig. S1†). The non-covalent wrapping interactions[52] between CAZ and **Fuc-AuNPs** and **Gal-AuNPs** were found to be stable over several days with no clear changes to both zeta potentials and the particle sizes (see ESI – Fig. S5†). Next, the phototherapeutic (PDT and PTT) properties of these systems were evaluated. 600 nm was chosen as the excitation wavelength for PDT/PTT experiments as this is the maximum absorption wavelength of **Fuc-AuNPs**/**Gal-AuNPs**. The known ROS fluorescent probe dihydrorhodamine was used to confirm ROS production upon light irradiation (600 nm, 1 W cm^{-2}). The ROS colorimetric probe tetramethylbenzidine (TMB) was used to confirm the production of ROS using UV-Vis spectroscopy.[53] Both **Fuc-AuNPs** and **Gal-AuNPs** were shown to produce ROS under light irradiation. No significant changes to ROS production were observed in the presence of lectins or by varying the pH and temperature (see ESI – Fig. S6†). Previous reports have shown the main ROS produced is $^1O_2$.[33,54] Interestingly, the light irradiation of UEA-1, AuNPs and **Fuc-AuNP@CAZ** displayed minimal PTT effects, however, upon lectin-binding a dramatic temperature increase was observed (see ESI – Fig. S7†). This observation is believed to be the result of the lectin-mediated formation of **Fuc-AuNP@CAZ** clusters allowing the generated heat to be localized, which enables an efficient increase in temperature. In contrast, when simple AuNPs are dispersed in solution, this results in a dissipation of the heat resulting in a poor PTT effect being observed. For **Fuc-AuNPs** and **Gal-AuNPs** in the presence of their corresponding lectins, a PTT conversion efficiency of 26.2% and 25.7% was observed respectively (see ESI – Fig. S8†). **Fuc-AuNP@CAZ** binding to *P. aeruginosa* (with LecA expression similar to UEA-1) was also shown to have a good PTT effect (see ESI – Fig. S9†). Demonstrating a potential mechanism of action, **Fuc-AuNP@CAZ** and **Gal-AuNP@CAZ** systems were shown to release CAZ gradually in the presence of either light irradiation or lectins (see ESI – Fig. S10 and S11†). No unwanted CAZ release was observed in their absence, which is in accordance with the stability data for **Fuc-AuNP@CAZ** and **Gal-AuNP@CAZ** systems (see ESI – Fig. S5†). According to these results, it is believed that the combined PDT and PTT effect will not only contribute to the overall therapeutic efficacy of CAZ towards *P. aeruginosa*, but also act as "triggers" to accelerate the release of co-loaded molecular cargos.

To confirm the LecB/LecA specificity and *P. aeruginosa* uptake of molecular cargos loaded on these glycoconjugate-based AuNPs, the fluorophore dicyanomethylene 4*H*-pyran (DCM) (see ESI† for chemical structure)[42] was loaded onto **Fuc-AuNPs**/**Gal-AuNPs**. In addition, this study was used to illustrate lectin binding from *P. aeruginosa* facilitates the release of the molecular cargo. Using a similar loading protocol, **Fuc-AuNPs** or **Gal-AuNPs** (0.8 nM) were mixed in an aqueous solution containing DCM (10 μM). Subsequent centrifugation (10 000 rpm) and washing (Tris-HCl buffer) afforded both **Fuc-AuNP@DCM** and **Gal-AuNP@DCM**. As seen in Fig. 3, *P. aeruginosa* (ATCC 27853) treated with either **Fuc-AuNP@DCM** or **Gal-AuNP@DCM** displayed an obvious fluorescence emission signal, which suggested the uptake of the DCM. Confirming the LecB and LecA-mediated uptake of the NIR fluorophore, *P. aeruginosa* was pre-treated with either free L-fucose or D-galactose (10 mM). This led to a marked reduction in fluorescence emission intensity being observed. This was believed to be due to the pre-saturation of the lectin binding sites which prevented the binding and uptake of **Fuc-AuNP@DCM**/**Gal-AuNP@DCM**. Overall, our approach demonstrates the targeted release of molecular cargos in *P. aeruginosa*.

Next, we turned our attention towards the evaluation of the antibacterial efficacy of each glycoconjugate-based AuNPs with and without light irradiation (30 min, 600 nm, 1 W cm^{-2}). In this study, *P. aeruginosa* (ATCC 27853) and drug-resistant *P. aeruginosa* (ATCC BAA2110) were treated with CAZ only, **Fuc-AuNPs**, **Gal-AuNPs**, **Fuc-AuNP@CAZ**, and **Gal-AuNP@CAZ**, respectively (Fig. 4). The sole use of CAZ (2 μg mL^{-1}) resulted in a moderate inhibition with no additional effect seen under light irradiation (30 min, 600 nm, 1 W cm^{-2}). **Fuc-AuNPs** and **Gal-AuNPs** were shown to have no "dark" therapeutic effect, whereas, the light irradiation of **Fuc-AuNPs**/**Gal-AuNPs** displayed a modest therapeutic effect with a slightly greater efficacy compared to unmodified AuNPs (see ESI – Fig. S12†).

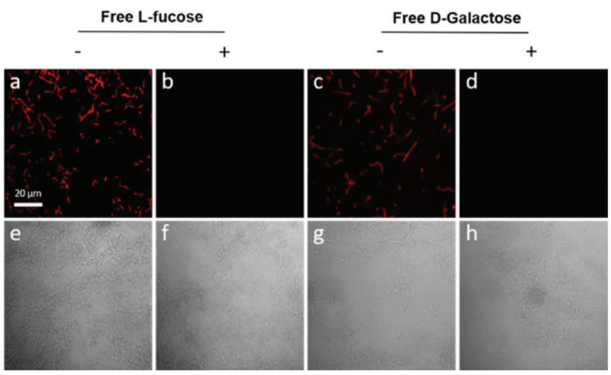

Fig. 3 Confocal Laser-Scanning Microscope (CLSM) images of *P. aeruginosa* (ATCC 27853): (a) **Fuc-AuNP@DCM** (0.2 nM and 1 μM) (b) pre-treatment with L-fucose (10 mM) followed by addition of **Fuc-AuNP@DCM** (0.2 nM and 1 μM) (c) **Gal-AuNP@DCM** (0.2 nM and 1 μM) (d) pre-treatment with D-galactose (10 mM) followed by addition of **Gal-AuNP@DCM** (0.2 nM and 1 μM) (e–h) bright field images of (a–d).

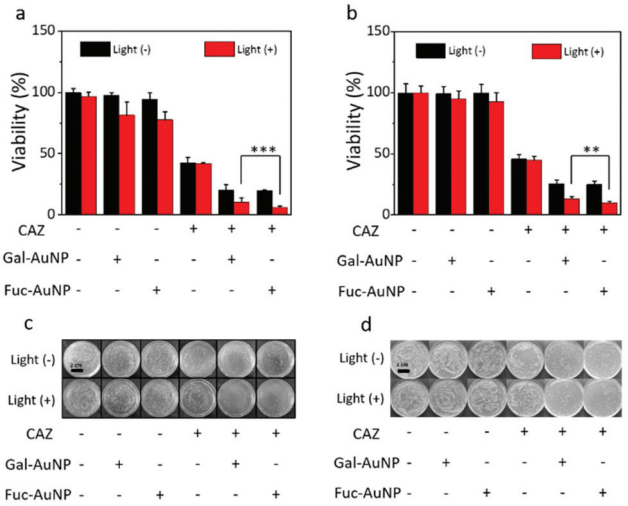

Fig. 4 (a) Relative viabilities of *P. aeruginosa* (ATCC 27853) treated with sterile water (control), **Fuc-AuNPs** (0.2 nM), **Gal-AuNPs** (0.2 nM), Ceftazidime (CAZ, 2 μg mL^{-1}), **Fuc-AuNP@CAZ** (0.2 nM and 2 μg mL^{-1}), and **Gal-AuNP@CAZ** (0.2 nM and 2 μg mL^{-1}) with and without light irradiation (30 min, 600 nm, 1 W cm^{-2}). (b) Relative viabilities of drug-resistant *P. aeruginosa* (ATCC BAA2110) treated with sterile water (control), **Fuc-AuNPs** (0.2 nM), **Gal-AuNPs** (0.2 nM), Ceftazidime (CAZ, 2 μg mL^{-1}), **Fuc-AuNP@CAZ** (0.2 nM and 2 μg mL^{-1}), and **Gal-AuNP@CAZ** (0.2 nM and 2 μg mL^{-1}) with and without light irradiation (30 min, 600 nm, 1 W cm^{-2}). (c) *P. aeruginosa* (ATCC 27853) colonies on Luria–Bertani (LB) agar plates treated with the respective systems with and without light irradiation (30 min, 600 nm, 1 W cm^{-2}). (d) *P. aeruginosa* (ATCC BAA2110) colonies on Luria–Bertani (LB) agar plates treated with the respective systems with and without light irradiation (30 min, 600 nm, 1 W cm^{-2}) ***$P < 0.001$; **$P < 0.01$.

The drug delivery capability of **Fuc-AuNPs** and **Gal-AuNPs** were confirmed with an enhanced therapeutic effect seen in comparison to CAZ. Remarkably, **Fuc-AuNP@CAZ** and **Gal-AuNP@CAZ** under light irradiation (30 min, 600 nm, 1 W cm^{-2}) demonstrated a significant cooperative therapeutic effect with CAZ, which almost resulted in full eradication (≈90%) (Fig. 4). This cooperative therapeutic effect was further confirmed using a LIVE/DEAD cell viability assay (see ESI – Fig. S13†). HR-TEM images were used to demonstrate the mode of action with **Fuc-AuNP@CAZ** initially interacting on the surface of *P. aeruginosa* and the subsequent light irradiation (30 min, 600 nm, 1 W cm^{-2}) resulting in a clear change to the morphology of the bacteria (see ESI – Fig. S14†). Confirming the selectivity for *P. aeruginosa*, the treatment of *E. coli* and methicillin-resistant *S. aureus* with **Fuc-AuNP@CAZ**/**Gal-AuNP@CAZ** were shown to have a significantly lower therapeutic outcome (see ESI – Fig. S15†). No toxicity was observed towards both 293T (human renal epithelial) and MDA-MB-231 (human breast cancer) cells (see ESI – Fig. S16†).

To demonstrate the full therapeutic potential of our glycoconjugate-based AuNPs strategy, *P. aeruginosa* biofilms were established on glass slides and steel surfaces. In these experiments, the performances were evaluated using the LIVE/DEAD biofilm viability assay (PI, dead – yellow and Syto9®, live –

blue). As shown in the processed 3D images of *P. aeruginosa* biofilms (Fig. 5), the use of just CAZ led to a partial antibiofilm effect, however, when co-loaded with **Fuc-AuNPs** or **Gal-AuNPs**, an enhanced antibiofilm effect was observed. Remarkably, light irradiation (600 nm, 30 min, 1 W cm^{-2}) of **Fuc-AuNP@CAZ**/**Gal-AuNP@CAZ** resulted in almost complete biofilm destruction on both glass slides and on clinically relevant steel surfaces (Fig. 5). Overall, this illustrates the potential of **Fuc-AuNP@CAZ**/**Gal-AuNP@CAZ** as excellent light and chemo-based antimicrobials for the targeted treatment of *P. aeruginosa*.

In summary, fucose and galactose-based glycoconjugated AuNPs (**Fuc-AuNPs** and **Gal-AuNPs**) were developed using a simple one-pot self-assembly procedure. Both **Fuc-AuNPs** and **Gal-AuNPs** displayed selective lectin-binding properties as determined by UV-Vis, HR-TEM and DLS analysis. The **Fuc-AuNPs** and **Gal-AuNPs** targeting ligands were effective for the selective carbohydrate-based recognition of *P. aeruginosa* key virulence factors, LecB/LecA. DCM-loaded **Fuc-AuNPs**/**Gal-AuNPs** afforded a highly selective bacterial fluorescence imaging agent.[55] While, CAZ loaded **Fuc-AuNPs**/**Gal-AuNPs** were shown to have improved therapeutic efficacy towards *P. aeruginosa* when compared to CAZ alone. Exploiting the phototherapeutic properties of the AuNP core (PTT and PDT), light irradiation resulted in an enhanced therapeutic effect towards *P. aeruginosa* when combined with CAZ. Significantly our targeted photo/chemotherapeutics **Fuc-AuNP@CAZ**/**Gal-AuNP@CAZ** were able to eradicate *P. aeruginosa* biofilm formation on glass slides and clinically relevant steel surfaces, with biocompatibility fully confirmed among human cells. Therefore, we believe the ease of preparation (one-pot) and remarkable therapeutic effects observed using this AuNPs strategy, will encourage other groups to develop targeted therapeutic materials in order to combat the important and ever-worsening problem of antibiotic resistant bacteria.

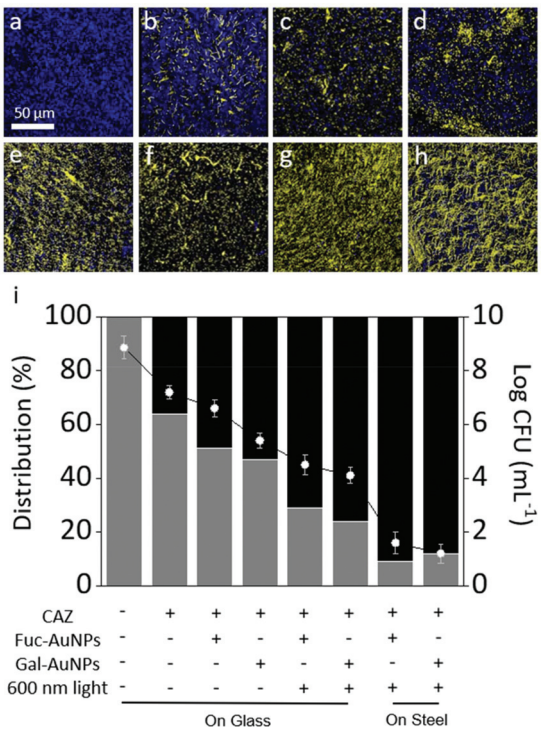

Fig. 5 The evaluation of **Fuc-AuNP@CAZ** and **Gal-AuNP@CAZ** for the treatment of biofilms. (a–f) Processed 3D images of *P. aeruginosa* biofilms on a glass-surface using the LIVE/DEAD biofilm viability assay. Dark experiments – (a) untreated (b) Cefazidime (CAZ) (32 μg mL^{-1}) (c) **Fuc-AuNP@CAZ** (0.2 nM and 32 μg mL^{-1}) (d) **Gal-AuNP@CAZ** (0.2 nM and 32 μg mL^{-1}) light experiments – (e) **Fuc-AuNP@CAZ** (0.2 nM and 32 μg mL^{-1}) (f) **Gal-AuNP@CAZ** (0.2 nM and 32 μg mL^{-1}) upon 30 min irradiation of 600 nm light (1 W cm^{-2}). (g and h) Processed 3D images of *P. aeruginosa* biofilms on steel surfaces using the LIVE/DEAD biofilm viability assay. (g) **Fuc-AuNP@CAZ**-treated (0.2 nM and 32 μg mL^{-1}) and (h) **Gal-AuNP@CAZ**-treated (0.2 nM and 32 μg mL^{-1}) groups upon 30 min irradiation of 600 nm light (1 W cm^{-2}). (i) Distributions of PI-stained (black, dead bacteria) and Syto9-stained (grey, live bacteria) *P. aeruginosa* biovolumes and CFU counts (white dots) of all above groups. Biovolume data are mean values of three independent replicates.

Conflicts of interest

There are no conflicts to declare.

Acknowledgements

The authors thank the NSFC (no. 91853201 and 21907030), the Shanghai Municipal Science and Technology Major Project (2018SHZDZX03), the National Key Sci-Tech Special Projects of Infection Diseases of China (2018ZX10732202), the International Cooperation Program of Shanghai Science and Technology Committee (17520750100) and the China Postdoctoral Science Foundation (2018M630407). TDJ wishes to thank the Royal Society for a Wolfson Research Merit Award.

References

1 L. R. Mulcahy, V. M. Isabella and K. Lewis, *Microb. Ecol.*, 2014, **68**, 1–12.
2 N. M. Maurice, B. Bedi and R. T. Sadikot, *Am. J. Respir. Cell Mol. Biol.*, 2018, **58**, 428–439.
3 D. Savoia, *Future Microbiol.*, 2014, **9**, 917–928.
4 C. I. Kang, S. H. Kim, H. B. Kim, S. W. Park, Y. J. Choe, M. D. Oh, E. C. Kim and K. W. Choe, *Clin. Infect. Dis.*, 2003, **37**, 745–751.
5 O. Ciofu and T. Tolker-Nielsen, *Front. Microbiol.*, 2019, **10**, 913, DOI: 10.3389/fmicb.2019.00913.
6 H. C. Flemming, J. Wingender, U. Szewzyk, P. Steinberg, S. A. Rice and S. Kjelleberg, *Nat. Rev. Microbiol.*, 2016, **14**, 563–575.
7 D. Nathwani, G. Raman, K. Sulham, M. Gavaghan and V. Menon, *Antimicrob. Resist. Infect. Control*, 2014, **3**, 32–48.
8 V. Aloush, S. Navon-Venezia, Y. Seigman-Igra, S. Cabili and Y. Carmeli, *Antimicrob. Agents Chemother.*, 2006, **50**, 43–48.

9 M. F. Moradali, S. Ghods and B. H. A. Rehm, *Front. Cell. Infect. Microbiol.*, 2017, **7**, 1–29.
10 A. Oliver, X. Mulet, C. Lopez-Causape and C. Juan, *Drug Resist. Updates*, 2015, **21–22**, 41–59.
11 X. L. Hu, N. Kwon, K. C. Yan, A. C. Sedgwick, G. R. Chen, X. P. He, T. D. James and J. Yoon, *Adv. Funct. Mater.*, 2020, **30**, 1907906.
12 Y. J. Liu, P. Bhattarai, Z. F. Dai and X. Y. Chen, *Chem. Soc. Rev.*, 2019, **48**, 2053–2108.
13 X. M. Sun, Z. Liu, K. Welsher, J. T. Robinson, A. Goodwin, S. Zaric and H. J. Dai, *Nano Res.*, 2008, **1**, 203–212.
14 B. Hu, L. P. Zhang, X. W. Chen and J. H. Wang, *Nanoscale*, 2013, **5**, 246–252.
15 S. Jeong, J. Lee, B. N. Im, H. Park and K. Na, *Biomaterials*, 2017, **141**, 243–250.
16 Z. H. Yu, X. S. Li, F. G. Xu, X. L. Hu, J. T. Yan, N. Kwon, G. R. Chen, T. T. Tang, X. J. Dong, Y. Y. Mai, D. J. Chen, J. Yoon, X. P. He and H. Tian, *Angew. Chem.*, 2020, **59**, 3658–3664.
17 Y. F. Ding, S. K. Li, L. J. Liang, Q. X. Huang, L. H. Yuwen, W. J. Yang, R. B. Wang and L. H. Wang, *ACS Appl. Mater. Interfaces*, 2018, **10**, 9980–9987.
18 Y. H. Feng, L. Liu, J. Zhang, H. Aslan and M. D. Dong, *J. Mater. Chem. B*, 2017, **5**, 8631–8652.
19 J. Zhang, Y. H. Feng, J. L. Mi, Y. T. Shen, Z. G. Tu and L. Liu, *J. Hazard. Mater.*, 2018, **342**, 121–130.
20 Q. Y. Chen, L. W. Zhang, Y. H. Feng, F. Shi, Y. B. Wang, P. Wang and L. Liu, *J. Mater. Chem. B*, 2018, **6**, 7643–7651.
21 J. Li, X. M. Liu, L. Tan, Z. D. Cui, X. J. Yang, Y. Q. Liang, Z. Y. Li, S. L. Zhu, Y. F. Zheng, K. W. K. Yeung, X. B. Wang and S. L. Wu, *Nat. Commun.*, 2019, **10**, 4490, DOI: 10.1038/s41467-019-12429-6.
22 C. Y. Mao, Y. M. Xiang, X. M. Liu, Z. D. Cui, X. J. Yang, Z. Y. Li, S. L. Zhu, Y. F. Zheng, K. W. K. Yeung and S. L. Wu, *ACS Nano*, 2018, **12**, 1747–1759.
23 C. Y. Mao, Y. M. Xiang, X. M. Liu, Z. D. Cui, X. J. Yang, K. W. K. Yeung, H. B. Pan, X. B. Wang, P. K. Chu and S. L. Wu, *ACS Nano*, 2017, **11**, 9010–9021.
24 X. Z. Xie, C. Y. Mao, X. M. Liu, L. Tan, Z. D. Cui, X. J. Yang, S. L. Zhu, Z. Y. Li, X. B. Yuan, Y. F. Zheng, K. W. K. Yeung, P. K. Chu and S. L. Wu, *ACS Cent. Sci.*, 2018, **4**, 724–738.
25 J. M. Zhang, Y. H. Sun, Y. Zhao, Y. L. Liu, X. H. Yao, B. Tang and R. Q. Hang, *Rare Met.*, 2019, **38**, 552–560.
26 C. F. Wang, J. Li, X. M. Liu, Z. D. Cui, D. F. Chen, Z. Y. Li, Y. Q. Liang, S. L. Zhu and S. L. Wu, *Biomater. Sci.*, 2020, **8**, 4216–4224.
27 K. Xiong, J. Li, L. Tan, Z. D. Cui, Z. Y. Li, S. L. Wu, Y. Q. Liang, S. L. Zhu and X. M. Liu, *Colloid Interface Sci. Commun.*, 2019, **33**, 100201.
28 S. Rana, A. Bajaj, R. Mout and V. M. Rotello, *Adv. Drug Delivery Rev.*, 2012, **64**, 200–216.
29 V. Maggi, F. Bianchini, E. Portioli, S. Peppicelli, M. Lulli, D. Bani, R. Del Sole, F. Zanardi, A. Sartori and R. Fiammengo, *Chem. – Eur. J.*, 2018, **24**, 12093–12100.
30 D. N. Heo, D. H. Yang, H. J. Moon, J. B. Lee, M. S. Bae, S. C. Lee, W. J. Lee, I. C. Sun and I. K. Kwon, *Biomaterials*, 2012, **33**, 856–866.
31 H. Y. Lee, K. A. Mohammed and N. Nasreen, *Am. J. Cancer Res.*, 2016, **6**, 1118–1134.
32 M. F. Attia, N. Anton, J. Wallyn, Z. Omran and T. F. Vandamme, *J. Pharm. Pharmacol.*, 2019, **71**, 1185–1198.
33 S. J. Chadwick, D. Salah, P. M. Livesey, M. Brust and M. Volk, *J. Phys. Chem. C*, 2016, **120**, 10647–10657.
34 M. U. Farooq, V. Novosad, E. A. Rozhkova, H. Wali, A. Ali, A. A. Fateh, P. B. Neogi, A. Neogi and Z. M. Wang, *Sci. Rep.*, 2018, **8**, 2907.
35 R. Vankayala, C. C. Lin, P. Kalluru, C. S. Chiang and K. C. Hwang, *Biomaterials*, 2014, **35**, 5527–5538.
36 S. M. Lee, H. J. Kim, Y. J. Ha, Y. N. Park, S. K. Lee, Y. B. Park and K. H. Yoo, *ACS Nano*, 2013, **7**, 50–57.
37 Y. Cheng, A. C. Samia, J. D. Meyers, I. Panagopoulos, B. W. Fei and C. Burda, *J. Am. Chem. Soc.*, 2008, **130**, 10643–10647.
38 J. D. Meyers, Y. Cheng, A. M. Broome, R. S. Agnes, M. D. Schluchter, S. Margevicius, X. N. Wang, M. E. Kenney, C. Burda and J. P. Basilion, *Part. Part. Syst. Charact.*, 2015, **32**, 448–457.
39 H. B. Mu, J. J. Tang, Q. J. Liu, C. L. Sun, T. T. Wang and J. Y. Duan, *Sci. Rep.*, 2016, **6**, 18877, DOI: 10.1038/srep18877.
40 M. C. Plotkowski, M. Chevillard, D. Pierrot, D. Altemayer, J. M. Zahm, G. Colliot and E. Puchelle, *J. Clin. Invest.*, 1991, **87**, 2018–2028.
41 A. V. Grishin, M. S. Krivozubov, A. S. Karyagina and A. L. Gintsburg, *Acta Nat.*, 2015, **7**, 29–41.
42 H. Y. Yang, J. J. Zhang, Y. Zang, H. Y. Zhang, J. Li, G. R. Chen and X. P. He, *Dyes Pigm.*, 2017, **136**, 224–228.
43 D. M. Richards and R. N. Brogden, *Drugs*, 1985, **29**, 105–161.
44 L. Y. Liang and D. Astruc, *Coord. Chem. Rev.*, 2011, **255**, 2933–2945.
45 S. Singh, I. S. Dubinsky-Davidchik and R. Kluger, *Org. Biomol. Chem.*, 2016, **14**, 10011–10017.
46 J. C. Love, L. A. Estroff, J. K. Kriebel, R. G. Nuzzo and G. M. Whitesides, *Chem. Rev.*, 2005, **105**, 1103–1169.
47 X. P. He, X. L. Hu, H. Y. Jin, J. M. Gan, H. L. Zhu, J. Li, Y. T. Long and H. Tiant, *Anal. Chem.*, 2015, **87**, 9078–9083.
48 T. T. Lou, Y. Q. Wang, J. H. Li, H. L. Peng, H. Xiong and L. X. Chen, *Anal. Bioanal. Chem.*, 2011, **401**, 333–338.
49 V. Chegel, O. Rachkov, A. Lopatynskyi, S. Ishihara, I. Yanchuk, Y. Nemoto, J. P. Hill and K. Ariga, *J. Phys. Chem. C*, 2012, **116**, 2683–2690.
50 X. Wang, O. Ramstrom and M. D. Yan, *J. Mater. Chem.*, 2009, **19**, 8944–8949.
51 P. Arbos, M. Wirth, M. A. Arangoa, F. Gabor and J. M. Irache, *J. Controlled Release*, 2002, **83**, 321–330.

52 X. L. Hu, L. Y. Chu, X. J. Dong, C. R. Chen, T. T. Tang, D. J. Chen, X. P. He and H. Tian, *Adv. Funct. Mater.*, 2019, **29**, 1806986, DOI: 10.1002/adfm.201806986.
53 R. Bresolí-Obach, M. Frattini, S. Abbruzzetti, C. Viappiani, M. Agut and S. Nonell, *Sensors*, 2020, **20**, 5952.
54 R. Vankayala, A. Sagadevan, P. Vijayaraghavan, C. L. Kuo and K. C. Hwang, *Angew. Chem., Int. Ed.*, 2011, **50**, 10640–10644.
55 W.-T. Dou, Z.-Y. Qin, J. Li, D.-M. Zhou and X.-P. He, *Sci. Bull.*, 2019, **64**(24), 1902–1909.